Application of minielectrochemical cell to corrosion studies of welded joints of austenitic stainless steel

F. Martín*[1], C. García[2], P. Tiedra[2], Y. Blanco[2] and M. López[2]

A specific electrochemical cell for small scale electrochemical testing has been built. The electrochemical cell has been made bearing in mind the microstructural features of the stainless steel weldments and the performance of the design has been verified. Two polarisation methods (potentiodynamic anodic polarisation measurements and cyclic potentiodynamic polarisation measurements) and two reactivation electrochemical techniques (the electrochemical potentio-kinetic reactivation test, EPR, and electrochemical potentio-kinetic reactivation double loop test, EPRDL) have been applied to two austenitic stainless steels: AISI 304 and AISI 316L. The results are reliable and have been compared to large scale experiments. Scanning of the welding joints has been performed and the results have been correlated with their microstructural features. It, thus, makes it possible to study the intrinsic heterogeneous microstructures such as the heat affected zone of a welded joint.

Keywords: Austenitic stainless steel, Intergranular corrosion, Pitting, Minicell, Welding

Introduction

There are a number of corrosion processes such as pitting, intergranular corrosion, stress corrosion cracking, crevice corrosion or galvanic corrosion which have been studied mainly based on large scale experiments with exposed areas in the mm^2–cm^2 range. However, such processes are due to mechanisms on a small scale. Therefore, it is advisable to develop appropriate small scale experimental devices that must necessarily undergo a thorough reduction of the exposed surface area of the working electrode. Additionally, these experimental devices can also be applied to other cases where an intrinsic heterogeneous material is the focus of interest. Clearly, the latter point applies to the study of welded joints.

Despite the numerous studies of localised corrosion processes on passive metal weldments, there are some unresolved aspects related to the local activation process. One of the reasons for this is due to the fact that standard electrochemical techniques are based on large scale experiments.[1–5] These methods do not allow inspection of the electrochemical behaviour of single heterogeneities associated with welded joints, such as dendritic segregation, precipitation of secondary phases, formation of unmixed zones, recrystallisation and grain growth in the heat affected zone (HAZ), volatilisation of alloying elements from the molten weld pool and contamination of the solidifying weld pool. Consequently, electrochemical methods which use miniature cells for investigating singles zones of special interest are, nowadays, a powerful tool.

A welded joint often presents critical corrosion behaviour. In the case of austenitic stainless steels, the corrosion behaviour has been evaluated[6] with standard practices such as ASTM A262, G48 and so forth. These methods provide general information that is quite acceptable in terms of comparative studies. However, they are incapable of separately studying the very different zones of a welded joint. Furthermore, large scale electrochemical tests such as ASTM G5 or G108 have been very successfully applied to the study of base materials but not for weldments. An alternative procedure has been the use of a lacquer coating to select a reduced, exposed area of the different weldment zones.[7,8] However, the results are not as good as with small scale electrochemical cells.

This work attempts to make a contribution to this challenging problem. The application of an electrochemical cell, appropriate in size and different to the capillary based microcells, is the main object of this work. The exposed size of this henceforth called ''minielectrochemical cell'' is within the range of about 1000–600 μm, which can be considered acceptable for the use of electrochemical techniques in the study of welded zones. Moreover, the comparative study of small and large scale experiments will help improve the understanding of repassivation kinetics.[9]

[1]Catedrático EU, Ciencia de Materiales e Ingeniería Metalúrgica, Universidad de Valladolid, Francisco Mendizabal s/n, Valladolid 47014, Spain
[2]Materials Engineering, E.T.S.I.I., Universidad de Valladolid. C/ Paseo del Cauce s/n, Valladolid 47011, Spain

*Corresponding author, email fmp@eis.uva.es;

Published by Maney on behalf of the Institute
Received 17 June 2007; accepted 21 October 2007
DOI 10.1179/17432780 8X286301

The use of small scale electrochemical cells, called microcells, is certainly not new, and since the mid 1990s several researchers have been developing studies based on their design.[10–17] Most of them are capillary based droplet cells, except that presented by Vogel and Schultze[15] which allows the continuous flow of electrolyte, optical control and temperature regulation. Nowadays, capillary microcells are well established in electrochemical surface analysis, including corrosion.

The main benefit of using microcells is directly related to the small size of the exposed working area,[18] which is in the micrometre range, although some drawbacks for capillary microcells must be considered, as has been explained by Birbilis *et al.*[19] To study welded joints, it would be possible to use this type of microcells whenever the capillary is large enough (for example 700 μm for tip size). However, even in this case, the electrolyte can not flow through the capillary cell and causes some drawbacks in its use.[19] To find a solution to these shortcomings, we here present a specific small scale electrochemical cell for corrosion studies which has been designated as a minicell.

The corrosion studies in this work have been performed on austenitic stainless steels. The main aspects related to these materials involve pitting corrosion and the degree of susceptibility (DOS) to sensitisation. Therefore, the electrochemical techniques used are potentiodynamic anodic polarisation, cyclic potentiodynamic polarisation measurements, the electrochemical potentiokinetic reactivation test (EPR) and the electrochemical potentiokinetic reactivation double loop test (EPRDL).

Experimental procedures

Materials, heat treatments and welding procedure

The materials used in this work were two commercial grade stainless steels, AISI 304 and AISI 316L, a 4 mm thick rectangular plate. The chemical compositions obtained by emission spectroscopy were: AISI 304: Fe–0·07C–17·5Cr–9·15Ni–0·51Si–1·75Mn–0·1Cu–0·025P–0·007S; AISI 316L: Fe–0·03C–17·21Cr–10·27Ni–1·86Mo–0·36Si–1·34Mn–0·23Cu–0·030P–0·003S.

The heat treatments were as follows: an annealing solution of AISI 304 performed by heating at 1050°C for 15 min under a stream of argon before being water quenched; an annealing solution of AISI 316L performed at 1100°C for 60 min under a stream of argon before being water quenched; sensitisation heat treatment of AISI 304 carried out at 675°C for 15, 30 and 60 min and sensitisation of AISI 316L performed at 750°C for 6, 24 and 75 h, both under a stream of argon. These long periods of heat treatment are needed if they are expected to be sensitisation because its low carbon content and the positive influence of molybdenum on corrosion resistance makes AISI 316L a very stable material.

The weldments were prepared by a fully automatic metal inert gas (MIG) process with argon as the shield gas, no edge preparation, butt joint and AISI 308 as filler material.

Electrochemical techniques

Four electrochemical techniques were used: potentiodynamic anodic polarisation, cyclic potentiodynamic polarisation measurements, electrochemical potentiokinetic reactivation test (EPR) and electrochemical potentiokinetic reactivation double loop test (EPRDL). Three replicate tests of each working area were performed without observing significant discrepancies.

The potentiodynamic anodic polarisation curves were performed following ASTM standard G-5.[20] The surface preparation of the samples was made with No. 800 emery paper. The tests were carried out in an acid solution with chlorides containing 1 M H_2SO_4 + 5 N NaCl and a temperature of 30 ± 1°C.The experimental procedures of the tests were the following: 5 min delay at open circuit (OC) potential, 2 min anodic attack at −220 mV_{SCE} (saturated calomel electrode), then a delay of 2 min at V_{OC}, 1 min cathodic cleaning at −600 mV_{SCE}, a 5 min delay at OC potential and then an anodic potentiodynamic scan which started at 50 mV_{SCE} below V_{OC} until 1000 mV_{SCE}. The potential scan rate used was 50 mV/min.

The cyclic potentiodynamic polarisation curves were used according to ASTM standard G-61.[21] The specimens were polished up to a 1 μm diamond finish. The polarisation curves were recorded in 1 M H_2SO_4 + 5 N NaCl at room temperature. Before polarisation, the sample was immersed in the test solution for 1 h at V_{OC}. The electrode potential was scanned from V_{OC} at a sweep rate of 10 mV/min. When the current density reached 5 mA for the macrocell test and 75 μA for the minicell test, the scanning direction was reversed until V_{OC} in order to evaluate the repassivation tendency.

The EPR test was performed following ASTM standard G-108,[22] but since the results were shown to be dependent on the degree of surface preparation, electrochemical conditioning was carried out. This allows the authors to use a degree of surface preparation (No. 600 emery paper) which is less severe than in the established standard test. The electrolyte was 0·5 M H_2SO_4 + 0·01 M KCN and the test temperature 30 ± 1°C. The experimental parameters of the conditioning were the following: a delay of 5 min at open circuit potential, deaerated; an anodic attack −220 mV_{SCE}; a delay of 2 min V_{OC}; a cathodic cleaning to −600 mV_{SCE} for 1 min and a delay of 5 min V_{OC}. Passivation is accomplished by applying the potential to +200 mV for 2 min. The reactivation scan starts at 200 mV until 50 mV below the V_{OC} at the rate of 100 mV/min.

The EPRDL test was carried out following the test conditions proposed elsewhere.[23,24] The surface preparation of the sample was finished with a 1 μm diamond polish; the electrolyte was 0·5 M H_2SO_4 + 0·01 M KCN and the test temperature 30 ± 1°C. There were three stages in the test: a 5 min delay at the open circuit potential V_{OC} to determine corrosion potential; anodic polarisation scan from E_{corr} to a potential of 300 mV_{SCE}, in the passive range at a scanning rate of 100 mV/min and a cathodic reactivation scan from 300 mV_{SCE} to V_{OC}. The results of the test, expressed as the ratio of the current densities, I_r/I_a, and the charges, Q_r/Q_a, given in percentages, were used to evaluate the susceptibility to IGC or DOS. I_r and Q_r were the maximum reactivation current density and charge during reverse scanning and I_a and Q_a were the maximum passivation current density and charge during anodic scanning.

For large scale measurements, a conventional corrosion cell with three electrodes was used. The testing

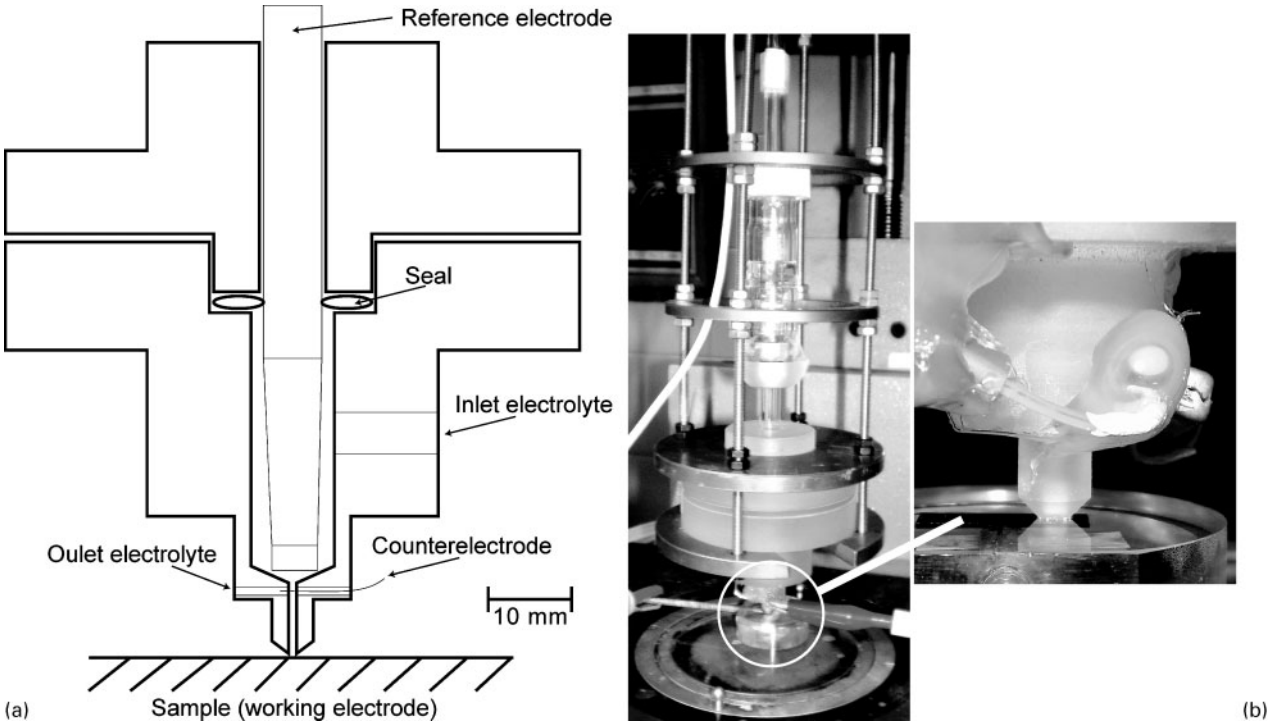

1 Schematic drawing and pictures of the minicell

specimen was used as the working electrode, two graphite rods as counter electrodes and an SCE equipped with a Luggin capillary as the reference electrode. The area of the working electrode was about 0·5 cm^2, which includes the complete section of the plate. Deaeration from 30 min before testing until the end of the test with nitrogen bubbling and stirring the electrolyte was used.

Description of minicell

The minicell made for this study had a size at the tip of 850 μm in diameter and was used to study the central section of the plates. Figure 1*a* shows the schematic drawing of the minicell and some real images are shown in Fig. 1*b*. To summarise, this is a cell made in PMMA. The electrolyte flows into the cell through the upper inlet (5 mm in diameter) and exits through the lower outlet (1 mm in diameter). Therefore, the reduction in the section causes a suction effect that renovates the chemical species of the working area and allows the continuous flow of the electrolyte over the working electrode area. The platinum counter electrode (0·2 mm wire) is positioned between the working and reference electrodes. The same reference electrode is used (saturated calomel electrode, SCE) as for large scale experiments and is located at a close distance to the working electrode (ca. 9 mm). Finally, there is no need to use a joint sealant on the tip of the cell: the PMMA already acts as a sealant and no leakage is observed. According to the sizes of the austenitic grains in the HAZ, the area of inspection could include about 1000 grains for AISI 304 (grain size parameter G=8) and 14 000 grains for AISI 316L (grain size parameter G=12).

Results and discussion

The main objectives were established in the introduction of this work. In the first part of this section some studies regarding the localised corrosion phenomena of non-welded austenitic stainless steels will be addressed. It will be concluded that the minicell gives results analogous to those obtained by means of a large scale electrochemical cell (i.e. a macrocell). In the second part, the welded joints of austenitic stainless steels will be the focus of interest.

Localised corrosion on sensitised austenitic stainless steels

Localised corrosion phenomena, such as pitting and intergranular corrosion, in sensitised austenitic stainless steels, are well established in the literature. Therefore, the main concern of this section is not to discuss that fact but to verify the proper functioning of the minicell. In other words, it is known[19] that the size of the working area in the microcells influences the experimental results and their interpretation. The electrolyte circulation also exerts an influence. Thus, it is necessary to perform some experimental runs with both the macro- and minicell to understand whether, with the minicell design, there are differences in the results or not.

With potentiodynamic anodic curves, it is possible to study both the general electrochemical behaviour of the materials as well as the pitting corrosion potential. The cyclic potentiodynamic curves provide information about pitting corrosion susceptibility and repassivation behaviour. These scanning techniques have, here, been applied to either AISI 304 or AISI 316L.

The shapes of the potentiodynamic anodic polarisation curves obtained with the minicell were coherent with the typical anodic polarisation plot. There was a satisfactory correlation between large and small scale measurements (Fig. 2). Current potential behaviours were very similar although there were some differences that, in fact, show the utility of applying the minicell to studying localised corrosion processes. Additionally, an anomalous behaviour was observed in relation to the

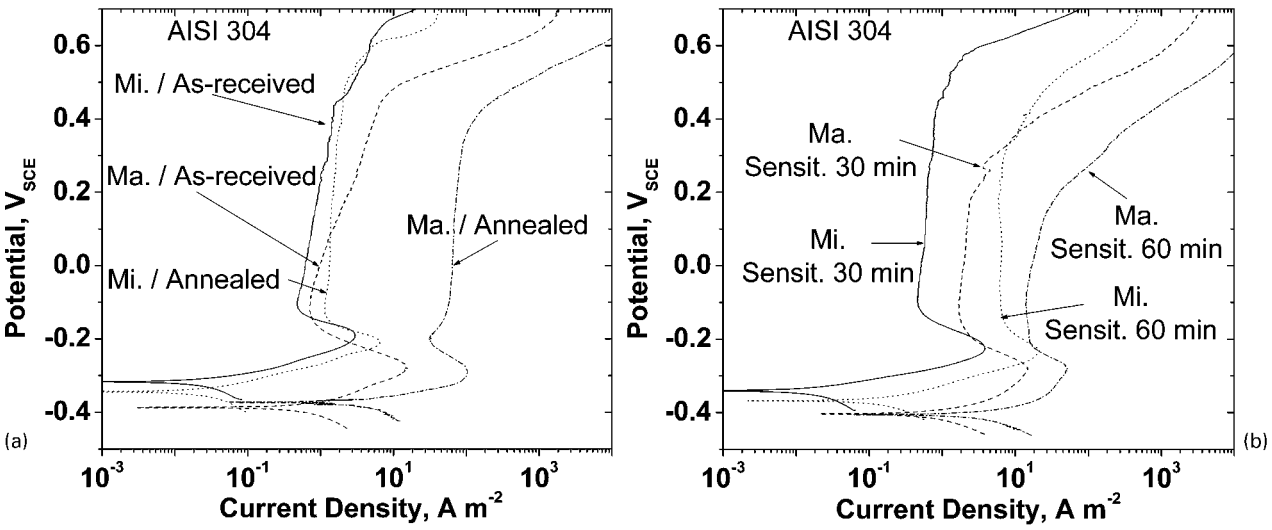

a as received and annealed solution samples; *b* samples sensitised at 675°C for 30 and 60 min

2 Polarisation scans performed by macro- and minicell set-ups for AISI 304

macrocell results. It was seen in Fig. 2*a* that the annealed material showed larger current densities than the as received material. This could be related to the coarsening of boundary grains as a consequence of carbon segregation[25] and/or to the precipitation of secondary phases rich in chromium originated by the high temperature of the solution annealing treatment.[26]

Electrochemical measurements on small sample areas indicate a better corrosion resistance than in large scale experiments.[27,28] In Fig. 2, some polarisation scans for AISI 304 performed by large and small scale experimental set-ups are shown. A slight shift can be observed to more noble potentials, lower current densities and a broader range of passivity when using the minicell. This could be explained in terms of a lower probability of including weak features on the working area as this diminishes. This fact has already been observed by Böhni *et al.*[29,30] The authors established that the pitting potential increases when the diameter of the microcell used decreases. This could also partially explain the fact that the greatest experimental differences between the macro- and minicell were found for sensitised samples, which show a higher density of local heterogeneities, such as second phase precipitates and subsequent chromium depleted zones. Furthermore, the fact must be considered that the materials investigated were commercial grades with some prior cold work in the superficial section and delta ferrite stringers in the central section. The presence of prior cold work is deleterious in terms of corrosion behaviour while the δ-ferrite shows a positive effect due to its high chromium content. For large scale experiments, the electrochemical measurements account for both phenomena, showing high current densities while, for the minicell, only the second phenomenon takes place.

When applying this polarisation method to AISI 316L, the results were consistent with those obtained above. In fact, this can be inferred from Fig. 3, which shows the polarisation scans performed by mini- and macrocell set-ups in annealed solution specimens and after sensitisation at 750°C for 6, 24 or 75 h. The differences observed between macro- and minicells for the annealed sample and also for the sample sensitised for 6 h (low degree of sensitisation) can be explained by

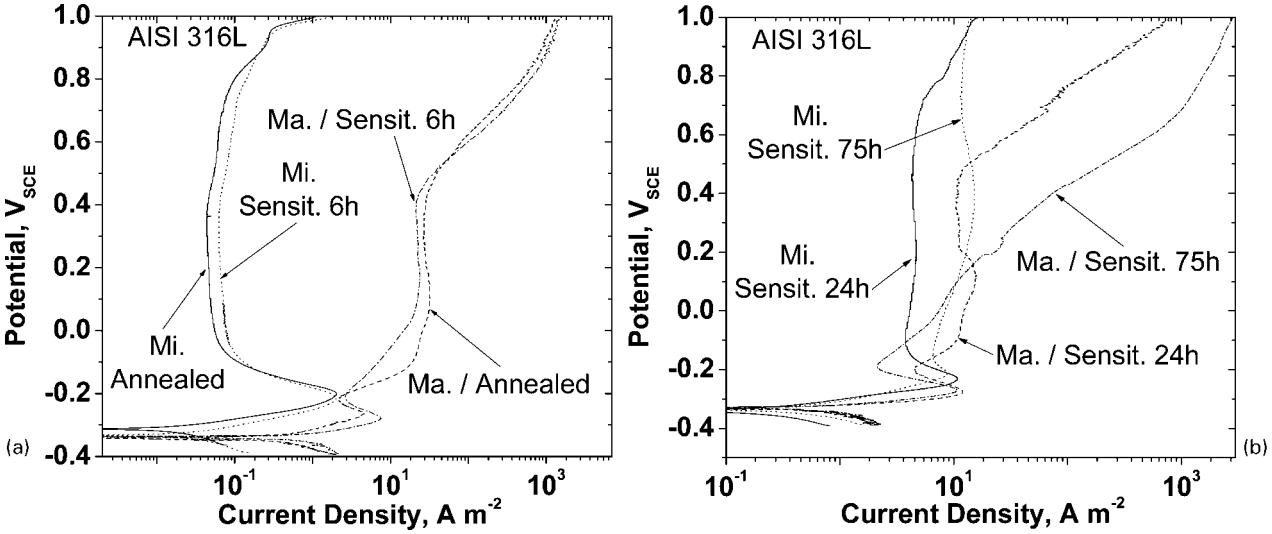

a at annealed solution state and after sensitisation at 750°C for 6 h; *b* after sensitisation at 750°C for 24 and 75 h

3 Polarisation scans performed by macro- and minicell set-ups for AISI 316L

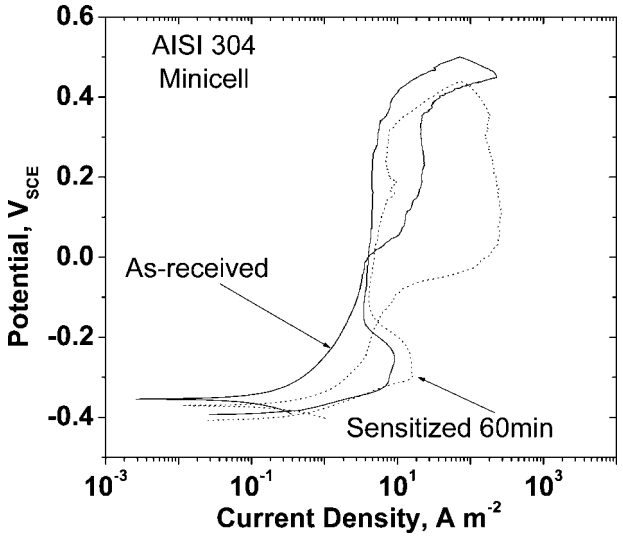

4 Cyclic potentiodynamic curves for AISI 304 and minicell set-up in as received state and after sensitisation at 675°C for 60 min

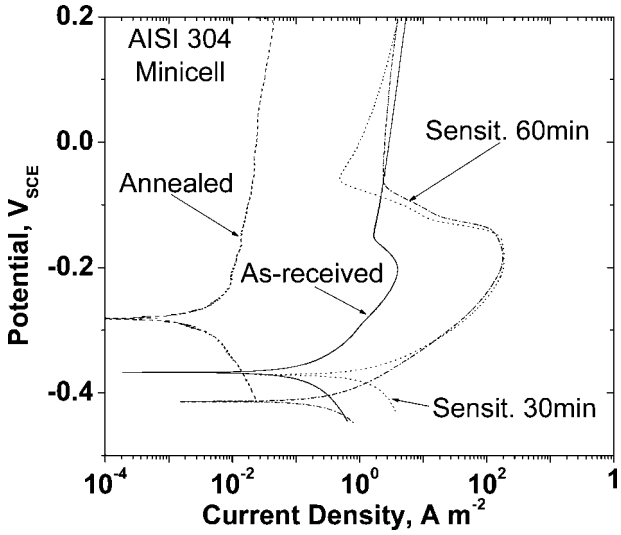

5 Curves of EPR for AISI 304 and minicell set-up in as received state, annealed solution state and after sensitisation at 675°C for 30 and 60 min

the same argument as for AISI 304 in the previous paragraph. For higher degrees of sensitisation (24 and 75 h), the additional fact of a much higher amount of chromium carbide precipitates in the whole section of the samples should be considered. Thus, current density differences between macro- and minicells are smaller. The negative effect of increasing sensitisation time is seen more clearly in the minicell experiments. An intense shift of the curves to the right and down can be observed, which means more negative corrosion potentials and higher current densities, either for i_{maximun} or for i_{passive}.

Since the potentiodynamic technique showed a good response, something similar was expected when using the cyclic potentiodynamic test. In fact, Fig. 4 shows the results after applying this technique to AISI 304 in as received and after sensitisation at 675°C for 60 min using the minicell set-up. The expected repassivation behaviour was observed, showing clearly the hysteresis anodic loops. The minicell was able to distinguish between the two different material states. After sensitisation, a higher repassivation current density was observed, a repassivation potential shifted to more negative values and a broader hysteresis loop. The sensitised material presented not only a much easier nucleation of pitting but also a higher pitting growth rate.

The EPR and EPRDL tests are particularly well suited for determining the susceptibility to intergranular corrosion but they can also help in the studies of other forms of localised corrosion.[31]

It is well known that EPR and EPRDL are the most useful scanning techniques for the assessment of the susceptibility to intergranular corrosion (IGC). These two techniques also have some significance on pitting and crevice corrosion measurements, as well as on SCC studies. Thus, there was special interest in knowing whether or not the minicell designed could be used for these techniques.

In trying to answer this question, the EPR reactivation curves for AISI 304 in as received state, in annealed solution state and in sensitisation state (675°C for 30 or 60 min) are collected in Fig. 5 — all of them obtained by means of the minicell. The results were as expected: an almost total absence of reactivation was observed, as well as a low current density for the annealed sample and a high susceptibility to intergranular corrosion on as-received and sensitised samples. Therefore, with the minicell, the positive effect of an annealed solution treatment and the negative effect of sensitisation heat treatments were verified.

When comparing these results to those obtained from the macrocell (Table 1), it can be seen that there is a good correlation of data. Although, absolute values are not coincident due to the effects of the exposure area size and the higher relative contributions of inhomogeneous sites from the large scale experimental set-up. Furthermore, as pointed out above, the negative effect

Table 1 Electrochemical data from EPR curves for AISI 304 in as received state and after sensitisation at 675°C for 30 or 60 min (macro- and minicell set-ups)

	Q_{react}*, C m^{-2}		I_{react}†, A m^{-2}		E_{corr}‡, V	
State	Minicell	Macrocell	Minicell	Macrocell	Minicell	Macrocell
As received	740	370	10·59	5·98	−0·362	−0·360
Sensitised 675°C, 30 min	10 030	28 330	142·20	447·70	−0·372	−0·425
Sensitised 675°C, 60 min	17 120	31 940	244·30	484·20	−0·407	−0·418

*Reactivation charge.
†Reactivation current density.
‡Corrosion potential.

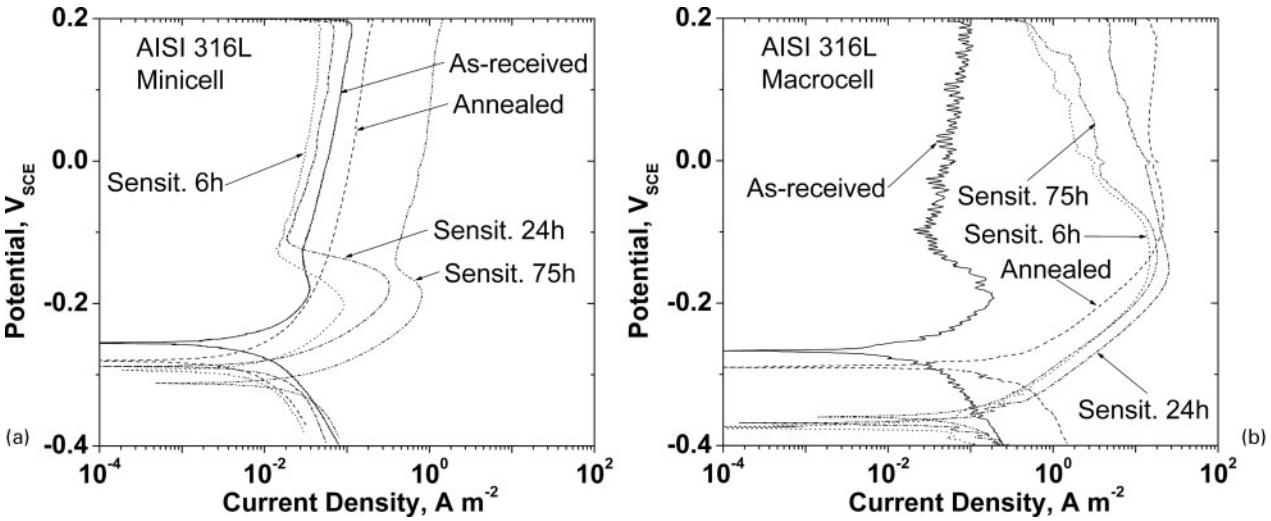

a minicell set-up; *b* macrocell set-up

6 Curves of EPR for AISI 316L in as received state, annealed solution state and after sensitisation at 750°C for 6, 24 or 75 h

of the prior cold work influencing when macrocell experiments are performed and the positive effect of δ-ferrite when using the minicell should not be forgotten. This last result is in agreement with previous conclusions obtained in polarisation studies, confirming the deleterious effect of the sensitisation heat treatment.

Also, the effect of the sensitisation time on IGC susceptibility was in agreement for both techniques, as can be observed in the charge reactivation data. The differences between the two sensitisation states (30 and 60 min) in terms of reactivation charge and current density were clearly evident for both experiments and were even more apparent for the minicell set-up.

The effects of the annealing and sensitisation treatment for AISI 316L were similar to those observed for AISI 304. As can be seen in Fig. 6, the reactivation curves were in good correlation between both experimental set-ups when sensitisation times were 6 and 24 h. For these degrees of sensitisation, the reactivation parameters increase as the time increases. However, two differences should be mentioned. First, a clearer difference was observed between the three states (annealing, sensitisation for 6 and 24 h) when the minicell was used. Second, on the annealed state, no reactivation was observed from the minicell set-up. Again, this could be related to the small size of the working area and the relatively minor amount of inhomogeneous sites where the passive film could be broken. The high resistance to the intergranular corrosion of this material might also help. The higher amount of δ-ferrite present in the working area when using the minicell might explain this beneficial effect. On the other hand, for the higher degree of sensitisation (75 h), the differences between mini- and macrocell set-ups are more remarkable. In macrocell measurements, the material exhibited lower reactivation current/charge than the one sensitised for 24 h. This healing was not observed with minicell measurements. Apart from the effect of the size of the working area, the different microstructures between the areas studied could justify these discrepancies. In fact, the prior cold work accelerates the sensitisation process and therefore the healing effect occurs for shorter sensitisation times.[32] In macrocell measurements, the zone studied covers the superficial area where prior cold work is present. Accordingly, chromium diffusion is facilitated and then the healing effect takes place. In minicell measurements, the zone studied is the inner part where there is no prior cold work and, thus, healing is delayed.

The cyclic measurements, such as the EPRDL test for macrocells, are generally used for assessing the susceptibility to intergranular corrosion in comparative terms. Initially, the results regarding the degree of sensitisation (DOS) should be better than those obtained by EPR, since it is a comparative technique and their results are independent of test conditions and the surface preparation of the samples. However, in some cases, lower sensibility has been observed and some difficulties were found in detecting low DOS.[31]

From the analysis of the EPRDL results collected in Fig. 7 for AISI 304, the following facts can be observed. When using the minicell, the absence of reactivation on the reverse scan of an as received state can be observed, but when using the macrocell set-up, although small, a slight reactivation took place. This might indicate that it is not advisable to reduce the exposure area very much, due to the loss of sensitivity associated with EPRDL. For sensitised simples (675°C for 60 min), the reverse sweep showed the typical reactivation related to chromium depletion. When evaluating the DOS, the small scale experimental set-up reflected even more differences between reactivation/passivation charges and current densities. Thus, again, it seems that the minicell might work properly with this technique, although some limitations related to low DOS should be considered.

To summarise, it can be said that the minicell functions properly and detects the different sensitisation states in austenitic stainless steels. Therefore, it is possible to apply this technique to the study of the welded joints of these materials with results reliable enough to draw valid conclusions.

Application of minicell to welded joints

The welded joints of AISI 304 and AISI 316L will be studied here. The main point of interest was to determine independently the DOS of the different zones

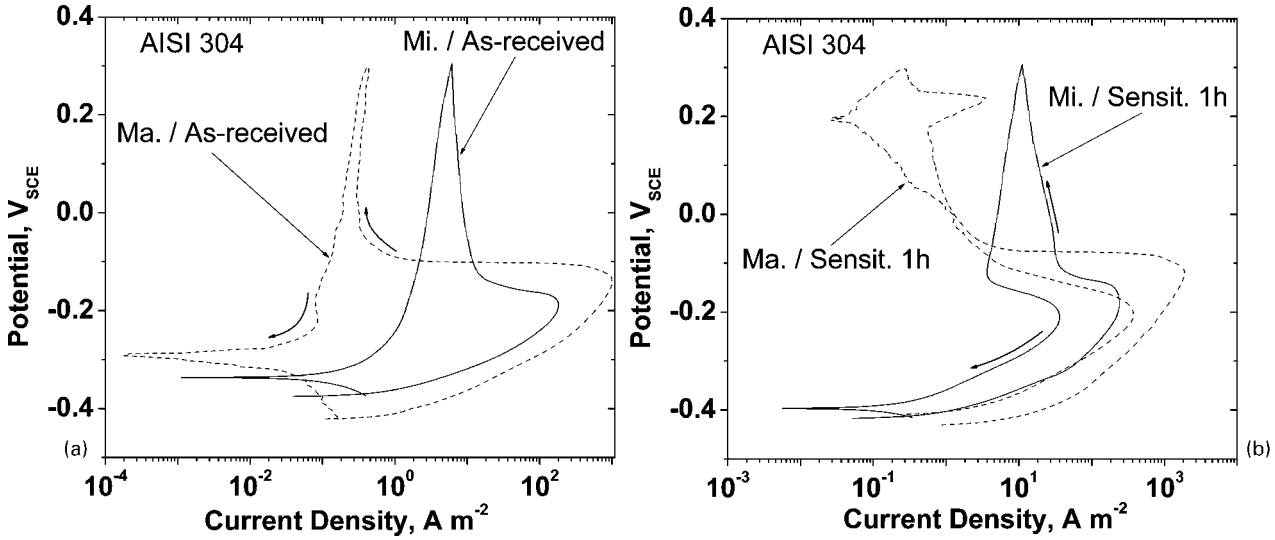

a in as received state; *b* after sensitisation at 675°C for 1 h

7 Curves of EPRDL for AISI 304 with macro- and minicell set-ups

of the welded joints. Regarding this issue, the minicell set-up has an important role in comparison with large scale set-ups because it allows the study of very different zones. The electrochemical techniques applied here were: the potentiodynamic anodic polarisation and EPR test. For the study of the sensitisation of the welded joints, it is not necessary to use cyclic potentiodynamic polarisation measurements and the EPRDL test, although it has been confirmed that they can be applied.

The material first chosen was AISI 304, in as received state which was subsequently welded. The intergranular susceptibility of this welded joint was investigated and, consequently, the EPR technique was selected. The reactivation behaviour of the following four zones was determined: weld metal, fusion line, HAZ and base material.

It can be observed in Fig. 8 how the weld metal does not reactivate: a continuous decrease was registered in the current density as the potential decreased. This could be interpreted as a sign of the high stability of the passive film to intergranular corrosion. The fact that the filler material is richer in chromium (AISI 308) in order to favour the presence of δ-ferrite and prevent hot cracking might be the reason for this stability of the passive film. This does not mean a lack of susceptibility to general corrosion or other corrosion mechanisms such as interdendritic corrosion.

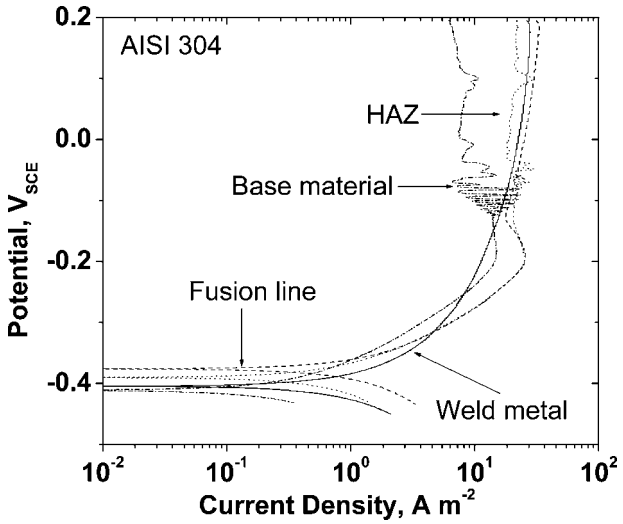

8 Curves of EPR for welded joint of AISI 304 scanned by minicell and in as received state: four different zones were examined (weld metal, fusion line, HAZ and base metal)

For the other three zones, the reactivation curves presented a passive current plateau. The fusion line showed a clear reactivation behaviour with high reactivation values (Q_r=2380 C m^{-2}, I_r=28 A m^{-2}). The HAZ (Q_r=3460 C m^{-2}, I_r=29 A m^{-2}) and the base material (Q_r=2230 C m^{-2}, I_r=20 A m^{-2}) showed a similar scan, although the latter showed the lowest reactivation values. In both cases, current oscillations were observed on the current density plateau. These current transients appeared when corrosion product layers began to be removed from the electrode surface and were interpreted as a sign of the breaking of corrosion products on the electrode surface. The charge and current density reactivation values increased, following the sequence: the base material lower than the fusion line and the fusion line lower than the HAZ.

For AISI 316L welded joint, no reactivation was observed after the EPR test in as received state and for every zone. As is well known, this steel shows better corrosion behaviour than AISI 304. Given this fact, and in order to verify the different electrochemical behaviour of the four welded joint zones, the AISI 316L was sensitised at 750°C for 6 h (Fig. 9). The EPR results are commented upon here. The weld metal zone showed a continuous decrease of current density as the potential decreased; the sensitisation heat treatment induced an abrupt increase in current density showing maximum current value and the corrosion potential shifted towards a less noble value. On the other hand, the other three zones exhibited clear reactivation scans with the base material showing minimum charge and current density reactivation values (Q_r=4·5 C m^{-2}, I_r=0·09 A m^{-2}). The HAZ reactivation scan was shifted towards less noble potential and higher current density with respect to the base material, while the charge and

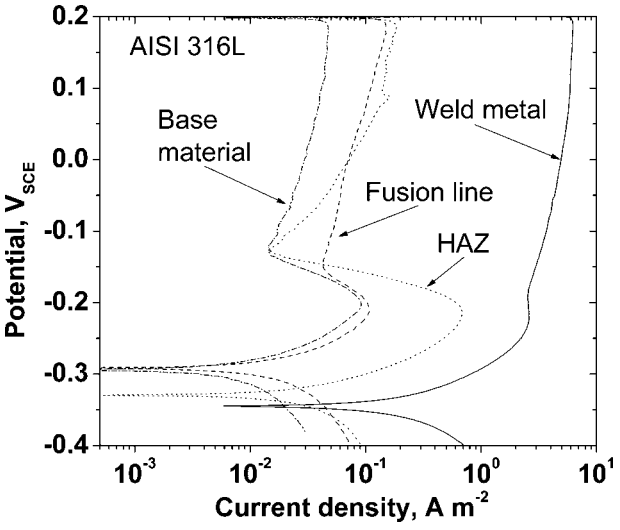

9 Curves of EPR for welded joint of AISI 316L scanned by minicell and after sensitisation at 750°C for 6 h: four different zones were examined (weld metal, fusion line, HAZ and base metal)

current density reactivation values were the highest (Q_r=36 C m^{-2}, I_r=0·68 A m^{-2}).

Figure 10 shows the microstructures of the different zones of the sensitised AISI 316L welded joint after the EPR test. The interdendritic attack on cast austenite grains was observed for the weld metal; the fusion line showed intergranular attack on austenitic grains and transgranular attack on austenite delta ferrite interface and the HAZ showed intense intergranular attack; the base material showed a much slighter intergranular attack and some transgranular attack on the austenite ferrite interface.

The reactivation scan of the AISI 316L weldment, sensitised at 750°C for 6 h, was also registered with a conventional macrocell: a lacquer coating was used to protect the untested area and only the part of the area containing a single welded zone was exposed to the corrosive electrolyte during measurements. The differences between the three zones analysed (weld metal, fusion line and HAZ) (Fig. 11) were much slighter than those observed using the minicell. The reactivation scan of the welded materials obtained by the macrocell set-up showed higher reactivation values as also happened in the verification test with non-welded materials. Current plateaus were not observed during the scanning process in the macroexperimental set-up. The weld metal and fusion line showed similar behaviour: this can be explained because of the inaccuracy of leaving a narrow zone uncovered. Nevertheless, both techniques agree in showing that the HAZ has the highest DOS.

The anodic polarisation measurements, using the minicell, are commented upon in the following paragraphs. The anodic behaviour of the AISI 316L welded sample in as received state is shown in Fig. 12. The weld metal and the fusion line showed a more stable passivity than the base material and the HAZ. However, they showed a higher anodic dissolution (I_{active}) and lower pitting corrosion potential ($E_{pitting}$). Corrosion potentials and corrosion current densities were obtained by Tafel analysis. The corrosion potentials for every zone showed slight differences and the base material was the

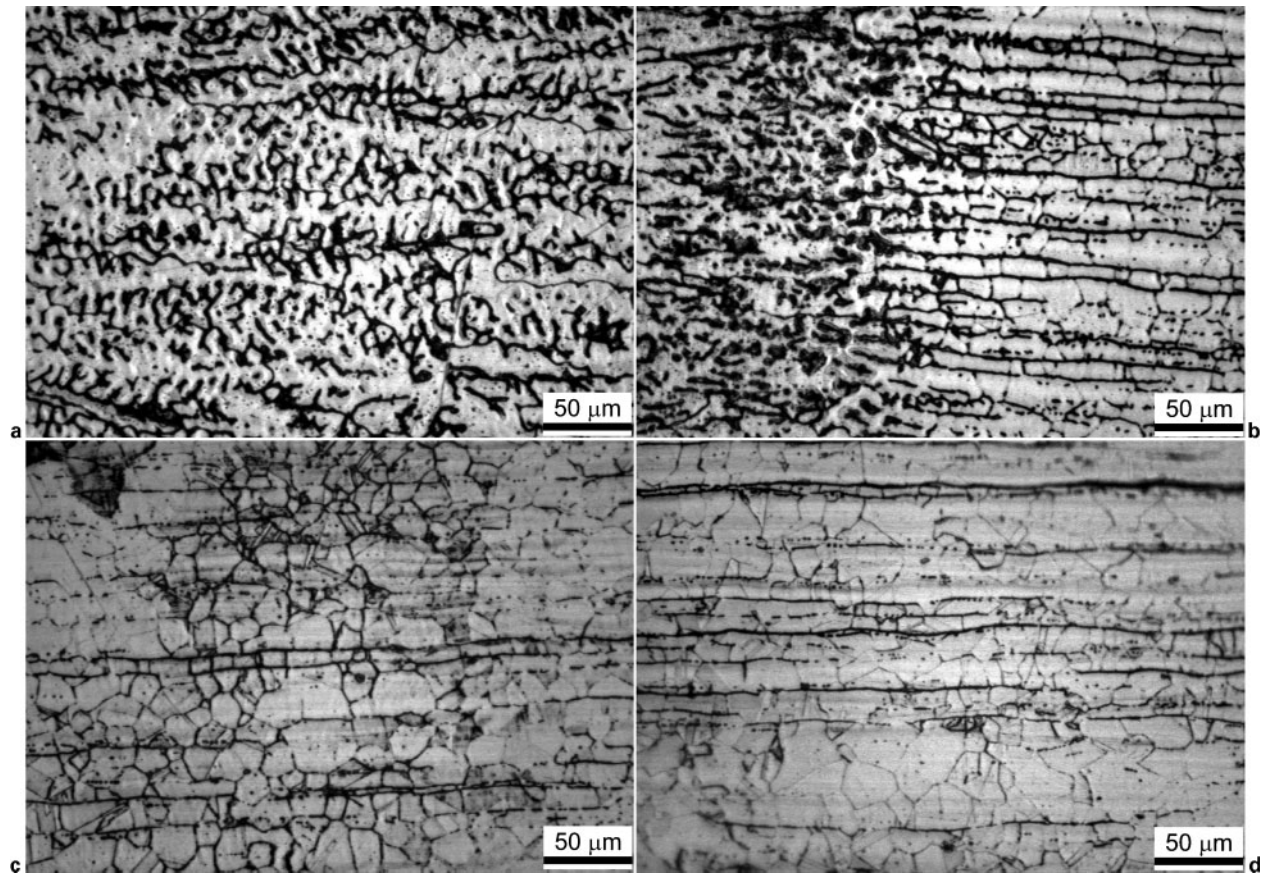

a weld metal; *b* fusion line; *c* HAZ; *d* base metal

10 Microstructures of welded joint zones of AISI 316L weldment after sensitisation at 750°C for 6 h and EPR test

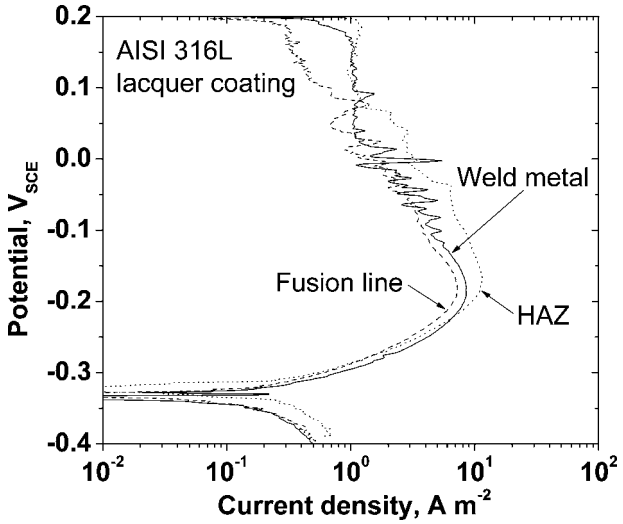

11 **Curves of EPR for welded joint of AISI 316L scanned by lacquer coating and after sensitisation at 750°C for 6 h**

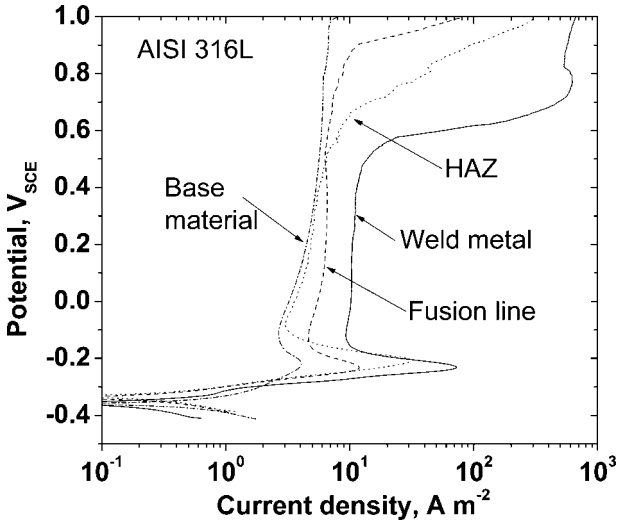

13 **Anodic polarisation measurements for welded joint of AISI 316L scanned by minicell and after sensitisation at 750°C for 6 h**

one exhibiting the noblest potential. With regard to corrosion current densities, the base material (1·6 mA m^{-2}) and the weld metal (2·1 A m^{-2}) exhibited lower values than the fusion line (4·1 A m^{-2}) and the HAZ (5·8 A m^{-2}). In all the cases, after testing, groups of small, globular pits were revealed by metallographic inspection.

Finally, after the sensitisation heat treatment at 750°C for 6 h (Fig. 13), it can be observed that the deleterious effect of sensitisation treatment was found to be notable for the weld metal and the HAZ while for the fusion line and the base material its anodic behaviour is analogous to the prior state. In fact, for the base material, the breakdown of the passive film occurred at very high values and the current densities were even lower than those registered without sensitisation. The fusion line still showed pitting potential and current densities of the same order as before. However, the sensitisation greatly affected the weld metal and the HAZ (pitting potentials of 0·484 V_{SCE} for the weld metal and 0·547 V_{SCE} for the HAZ). Additionally, a considerable increment of active and passive current densities for the weld metal was observed. Therefore, this was the order of susceptibility to pitting corrosion. The negative effect of sensitisation treatment was again verified and this could be related to the microstructural aging of the δ-ferrite which, as said before, is highly present in the weld metal. The anodic behaviour of the fusion line was intermediate between the weld metal and the base material. In fact, the most voluminous pitting was localised in the weld metal zone. The HAZ and base material continued to show similar electrochemical behaviour but the sensitisation had an important effect on the HAZ. Comparative analysis indicated that the sensitised HAZ showed higher anodic current density, a broader active–passive transition potential range and a minimum passive potential range. Thus, it is a critical zone which is susceptible to localised corrosion.

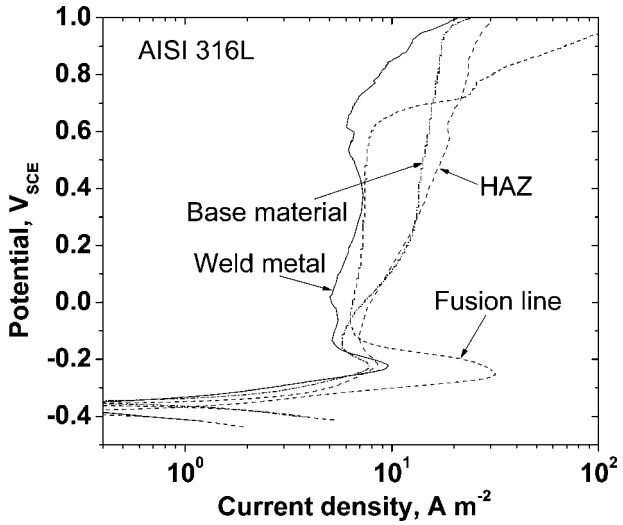

12 **Anodic polarisation measurements for welded joint of AISI 316L scanned by minicell and in as received state**

These are introductory studies which in the future will be extensively developed. Nevertheless, the capacity of the minicell used in this work is clearly demonstraded. It is worth mentioning that the size of the exposure area does not always have to be as small as possible, since it depends on the field of interest. In fact, in welded joints, when the object is to relate microstructural features to corrosion behaviour, an excessively small exposure area would hide the facts sought.

Conclusions

The minicell used in this work operates properly and is capable of detecting the different sensitisation states in austenitic stainless steels. Therefore, it is possible to apply this device to the study of the welded joints of these materials, and the results are reliable enough to draw valid conclusions. The electrochemical techniques which can be applied are polarisation measurements and reactivation electrochemical techniques.

When these kinds of experimental devices are used, the results should be analysed bearing in mind that the areas inspected are small in size and that contributions from very heterogeneous zones can be found. This is the reason why it is advisable to establish a correlation by

direct microstructural observation. The application of the minicell to welded joints is promising because it can reveal various electrochemical details of the different zones of a welded joint. It has been observed that the HAZ, for both AISI 304 and AISI 316L, is the most critical zone in relation to intergranular corrosion behaviour and this becomes clearer after post-welding sensitisation heat treatments. The weld metal and the fusion line are also susceptible to other types of localised corrosion. The base corrosion behaviour is shown to be that of the base material as expected and as was here verified with the minicell.

Thanks to the fact that the minicell inspects zone by zone, the results are shown to be very comprehensible. When different experimental devices are used, the results may be hidden or perhaps not so evident.

Acknowledgements

This work was funded by the Dirección General de Investigación, Ministerio de Educación y Ciencia, Spain, reference MAT2004-00354.

References

1. Z. Szlarska-Dmialowska: 'Pitting corrosion of metals', 145–157; 1986, Houston, TX, NACE International Publishers.
2. S. E. Lott and R. C. Alkire: *J. Electrochem. Soc*., 1989, **136**, 973–979.
3. C. Meadows and J. D. Fritz: *Weld. J.*, 2005, **7**, 26–30.
4. W. T. Tsai, C. L. Yu and J. I. Lee: *Scripta Mater.*, 2005, **53**, 505–509.
5. E. Blasco-Tamarit, A. Igual-Muñoz, J. Garcia-Anton and D. Gacia-Garcia: *Corros. Sci.*, 2006, **48**, 863–886.
6. A. H. Tuthill: *Weld. J.*, 2005, **5**, 36–40.
7. L. Reclaru, R. Lerf, P. Y. Eschler and J. M. Meyer: *Biomaterials*, 2001, **22**, 269–279.
8. B. T. Lu, Z.K.Chen, J. L. Luo, B. M. Patchett and Z. H. Xu: *Electrochim. Acta*, 2005, **50**, 1391–1403.
9. F. Assi and H. Böhni: *Wear*, 1999, **233–235**, 505–514.
10. H. Böhni, T. Suter and A. Schereyer: *Electrochim. Acta,* 1995, **40,** 1361–1368.
11. T. Suter and H. Böhni: *Electrochem. Soc. Proc.,* 1995, **9515**, 127–137.
12. A. W. Hassel and M. M. Lohrengel: *Electrochim. Acta*, 1997, **42**, 3327–3333.
13. M. M. Lohrengel: *Electrochim. Acta*, 1997, **42**, 3265–3271.
14. F. Assi and H. Böhni: *Wear*, 1999, **233–235**, 505–514.
15. A. Vogel and J. W. Schultze: *Electrochim. Acta*, 1999, **44**, 3751–3759.
16. R. Ambat, M. Jariyaboon, A. J. Davenport, S. W. Williams, D. A. Price and A. Wescott: Proc. of the 15th International Corrosion Congress, Granada, ICC (International Corrosion Council), Spain, 22–27 September, 2002.
17. J. O. Park, T. Suter and H. Böhni: *Corrosion*, 2003, **59,** (1), 59–67.
18. M. M. Lohrengel, C. Rosenkranz, I. Klüppel, A. Moehring, H. Bettermann, B. Van der Bossche and J. Deconinck: *Electrochim. Acta*, 2004, **49**, 2863–2870.
19. N. Birbilis, B. N. Padgett and R. G. Bucheit: *Electrochim. Acta*, 2005, **50**, 3536–3544.
20. ASTM Standard G-5-87: 'Standard reference test method for making potentiostatic and potentiodynamic anodic polarization measurements', 71–75; 1993, Philadelphia, ASTM.
21. ASTM Standard G61–86: 'Standard test method for conducting cyclic potentiodynamic polarization measurements for localized corrosion susceptibility of iron-nickel- or cobalt-based alloys', 239–243; 1993, Philadelphia, ASTM.
22. ASTM Standard G108-92: 'Standard test method for EPR for detecting sensitization of AISI Type 304 and 304L Stainless Steels', 457–463, Philadelphia, ASTM.
23. A. P. Majidi and M. A. Streicher: *Corrosion*, 1984, **40**, 584–593.
24. V. Čihal and R. Štefec: *Electrochim. Acta*, 2001, **46**, 3867–3877.
25. L. Colombier and J. Hochman: 'Stainless and heat resisting steels', 2nd edn; 1967, London, Edward Arnold Ltd.
26. J. L. Cavazos: *Mater. Charact.*, 2006, **56,** 96–101.
27. T. Suter and H. Böhni: *Electrochim. Acta*, 1998, **43**, 2843–2849.
28. R. A. Perren, T. A. Suter, P. J. Uggowitzer, L. Weber, R. Magdowski, H. Böhni and M. O. Speidel: *Corros. Sci.,* 2001, **43**, 707–726.
29. H. Böhni, T. Suter and A. Schreyer: *Electrochim. Acta*, 1995, **40**, 1361–1367.
30. H. Böhni, T. Suter and F. Assi: *Surf. Coat. Technol.*, 2000, **130**, 80–86.
31. V. Kain, K. Chandra, K. N. Adhe and P. K. De: *J. Nucl. Mater.*, 2004, **334**, 115–132.
32. C. García, F. Martin, P. de Tiedra, J. A. Heredero and M. L. Aparicio: *Corros. Sci.*, 2000, **56**, 243–255.